

Design and Flight Test of a Lateral-Directional Command Augmentation System

David Atzhorn* and Robert F. Stengel†

Princeton University Flight Research Laboratory, Princeton, New Jersey

Two-input/two-output, lateral-directional control laws with Type 0 and Type 1 structures have been designed, analyzed, and flight tested using the microprocessor-based digital flight control system (Micro-DFCS) installed in Princeton's Variable-Response Research Aircraft (VRA). These control laws were designed using linear-quadratic, sampled data regulator theory, and were evaluated by U.S. Navy test pilots. Major closed-loop response features were found to be relatively insensitive to sampling rate (down to 4 sps), although flying qualities were degraded by increased sampling delay. Type 0 controllers provided satisfactory performance in flight, but the equivalent Type 1 systems were found to be unduly sensitive to disturbances and measurement noise.

Introduction

MANY future aircraft will require command and stability augmentation to meet handling qualities requirements while achieving performance objectives. The reasons for this include increasing use of relaxed static stability margins, substantial variations in dynamic characteristics over expanded flight envelopes, and increasing workloads associated with more demanding missions. Modern control theory and digital microprocessors can be expected to play complementary roles in the development of such control systems. They provide both the method for designing complex control structures and the means for implementing them in flight. This paper presents the results of an analytical and experimental investigation of the application of modern control technology to lateral-directional command augmentation systems.

Linear-quadratic, sampled-data regulator theory was used to design several Type 0 and Type 1 digital control laws for the Variable-Response Research Aircraft (VRA). Lateral-directional control structures were defined for singular command inputs¹ and for control rate outputs. The former allows for precise following of a command variable whose integral appears in the state vector, while the latter provides either low-pass filtering or proportional-integral compensation of control outputs. CAS-4, the control program for the VRA's microprocessor-based digital flight control system (Micro-DFCS), offered four combinations of command/control structure: direct electrical linkage ("Digital DEL") from the lateral stick and foot pedals to the ailerons and rudder, Type 0 control with sideslip angle/roll rate and lateral acceleration/roll rate command inputs, and Type 1 control with sideslip angle/roll rate command. The Model 1 Micro-DFCS used the 8085 central processor in a Multibus architecture. CAS-4 was coded in assembly language using floating-point arithmetic and the general organization described in Refs. 2 and 3. Additional details of this investigation can be found in Ref. 4.

Digital Control Law Development

Aircraft Model and Design Objectives

Lateral-directional motions of an aircraft can be described by the fourth-order linear differential equation,

$$\Delta \dot{x} = F \Delta x + G \Delta u \quad (1)$$

The state vector, Δx , represents perturbations in yaw rate (Δr), sideslip angle ($\Delta \beta$), roll rate (Δp), and roll angle ($\Delta \phi$):

$$\Delta x^T = (\Delta r \ \Delta \beta \ \Delta p \ \Delta \phi) \quad (2)$$

The VRA can be controlled independently about all six degrees of freedom, as it is equipped with direct-lift and direct-side force surfaces in addition to its conventional controls. Longitudinal motions were not a subject for study (although they were, of course, controlled by the pilot in flight), and the VRA's side-force panels were not actively controlled in this program; hence, the control vector Δu considered here represents perturbations in rudder angle ($\Delta \delta R$) and aileron angle ($\Delta \delta A$) only:

$$\Delta u^T = (\Delta \delta R \ \Delta \delta A) \quad (3)$$

The corresponding stability and control matrices, F and G , are defined as in Ref. 5. Taking straight-and-level flight with an indicated airspeed of 105 kt as the nominal flight condition, the numerical values of the VRA's lateral-directional matrices are,

$$F = \begin{bmatrix} -.75 & 5.9 & -.26 & 0 \\ -1 & 0.4 & 0 & 0.18 \\ 1.16 & -11.5 & -6.5 & 0 \\ 0 & 0 & 1 & 0 \end{bmatrix} \quad (4)$$

$$G = \begin{bmatrix} -6.1 & -.25 \\ -.07 & 0 \\ .58 & 21 \\ 0 & 0 \end{bmatrix} \quad (5)$$

(All angles are measured in radians or degrees.)

Submitted Nov. 12, 1981; presented as Paper 81-2331 at the AIAA/IEEE 4th Digital Avionics Systems Conference, St. Louis, Mo., Nov. 17-19, 1981; revision submitted July 27, 1983. Copyright © American Institute of Aeronautics and Astronautics, Inc., 1981. All rights reserved.

*Captain, United States Air Force; formerly Graduate Student, Princeton University.

†Professor of Mechanical and Aerospace Engineering, Associate Fellow, AIAA.

Satisfying established specifications for handling qualities (e.g., Ref. 6) is a reasonable goal for designing an aircraft control system, and the present designs have been evaluated in this respect⁴; however, the "bare airframe" VRA falls well within the Level 1 requirements of Ref. 6, so this aircraft has no immediate need for command or stability augmentation. Recognizing that flight testing provides the unique ability to gather further evidence regarding just what handling qualities *are* satisfactory, we have chosen instead to examine a range of command modes and aircraft responses generally falling within Level 1 limits.

Sampled-Data Regulators and Equilibrium Response

Direct Digital Synthesis

This is used to design the command augmentation control laws, so it is necessary to define the discrete-time equivalent of Eq. (1)

$$\Delta \mathbf{x}_{k+1} = \Phi \Delta \mathbf{x}_k + \Gamma \Delta \mathbf{u}_k \quad (6)$$

The lateral-directional command augmentation system is designed as a sampled-data regulator, i.e., as a discrete-time (digital) controller that minimizes a continuous-time (analog) linear-quadratic cost function subject to a dynamic constraint [Eq. (8)]. The solution algorithms follow Refs. 7 and 8 with modifications, as described below.

As shown later in this section, the pilot's command input, $\Delta \mathbf{y}^*$, specifies equilibrium values of the state and control, $\Delta \mathbf{x}^*$ and $\Delta \mathbf{u}^*$, collectively known as the regulator set point. Perturbations from the set point are described by

$$\Delta \tilde{\mathbf{x}}(t) = \Delta \mathbf{x}(t) - \Delta \mathbf{x}^*(t) \quad (7)$$

$$\Delta \tilde{\mathbf{u}}(t) = \Delta \mathbf{u}(t) - \Delta \mathbf{u}^*(t) \quad (8)$$

Assuming that the set point is fixed, Eqs. (1) and (6) apply equally to the () variables, and the continuous-time cost function can be expressed as

$$J = \frac{1}{2} \sum_{k=0}^{\infty} \int_{t_k}^{t_{k+T}} \left\{ [\Delta \tilde{\mathbf{x}}^T(t) \Delta \tilde{\mathbf{u}}^T(t)] \begin{bmatrix} \mathbf{Q} & \mathbf{M} \\ \mathbf{M}^T & \mathbf{R} \end{bmatrix} \begin{bmatrix} \Delta \tilde{\mathbf{x}}(t) \\ \Delta \tilde{\mathbf{u}}(t) \end{bmatrix} \right\} dt \quad (9)$$

As in Ref. 8, minimization of this cost function leads to proportional (Type 0) command augmentation control

$$\Delta \tilde{\mathbf{u}}_k = -K \Delta \tilde{\mathbf{x}}_k \quad (10a)$$

$$\Delta \mathbf{u}_k = \Delta \mathbf{u}_k^* - K(\Delta \mathbf{x} - \Delta \mathbf{x}^*) \quad (10b)$$

We can formulate logic that drives the control *rate*, $\Delta \mathbf{v} = \Delta \dot{\mathbf{u}}$, rather than the control *displacement*. Then the control rate can be weighted in the cost function, providing a means for limiting high-frequency or rapid motions of the controls. The cost function and state equation are augmented as follows:

$$J = \frac{1}{2} \sum_{k=0}^{\infty} \left\{ [\Delta \tilde{\mathbf{x}}^T \Delta \tilde{\mathbf{u}}^T \Delta \tilde{\mathbf{v}}^T]_k \times \begin{bmatrix} \hat{\mathbf{Q}}_1 & \hat{\mathbf{M}} & \hat{\mathbf{N}}_1 \\ \hat{\mathbf{M}}^T & \hat{\mathbf{Q}}_2 & \hat{\mathbf{N}}_2 \\ \hat{\mathbf{N}}_1^T & \hat{\mathbf{N}}_2^T & \hat{\mathbf{R}} \end{bmatrix} \begin{bmatrix} \Delta \tilde{\mathbf{x}} \\ \Delta \tilde{\mathbf{u}} \\ \Delta \tilde{\mathbf{v}} \end{bmatrix}_k \right\} \quad (11)$$

$$\begin{bmatrix} \Delta \tilde{\mathbf{x}} \\ \Delta \tilde{\mathbf{u}} \end{bmatrix}_{k+1} = \begin{bmatrix} \Phi & \Gamma \\ 0 & I \end{bmatrix} \begin{bmatrix} \Delta \tilde{\mathbf{x}} \\ \Delta \tilde{\mathbf{u}} \end{bmatrix}_k + \begin{bmatrix} 0 \\ TI \end{bmatrix} \Delta \tilde{\mathbf{v}}_k \quad (12)$$

The () weighting matrices are derived from continuous-time weighting matrices as in {7}, and the perturbation control law

$$\Delta \tilde{\mathbf{v}}_k = -K_1 \Delta \tilde{\mathbf{x}}_k - K_2 \Delta \tilde{\mathbf{u}}_k \quad (13)$$

(it can be assumed that $\Delta \mathbf{v}^* = 0$; hence, $\Delta \tilde{\mathbf{v}} = \Delta \mathbf{v}$.) This can be transformed to control displacement logic using a forward-difference approximation for the derivative:

$$\Delta \tilde{\mathbf{v}}_k = (\Delta \tilde{\mathbf{u}}_{k+1} - \Delta \tilde{\mathbf{u}}_k) / T \quad (14)$$

Equation (13) becomes

$$\Delta \tilde{\mathbf{u}}_k = (I - TK_2) \Delta \tilde{\mathbf{u}}_{k-1} - TK_1 \Delta \tilde{\mathbf{x}}_{k-1} \quad (15)$$

The lagged $\Delta \eta$ feedback introduces low-pass filtering in this control. This can be expressed as the proportional filter (Type 0) command augmentation control law,

$$\Delta \mathbf{u}_k = \Delta \mathbf{u}_k^* + (I - TK_2) (\Delta \mathbf{u} - \Delta \mathbf{u}^*)_{k-1} - TK_1 (\Delta \mathbf{x} - \Delta \mathbf{x}^*)_{k-1} \quad (16)$$

For a step input and zero initial conditions, the initial control depends only on the steady-state value, $\Delta \mathbf{u}^*$; the cost function and its minimization have no effect until the next sampling instant.

An alternative approximation to the control derivative incorporates the effects of cost function minimization in the computation of the initial control. Taking the Laplace transform of Eq. (13) and combining terms yields,

$$(sI + K_2) \Delta \mathbf{u}_k(s) = -K_1 \Delta \tilde{\mathbf{x}}_k(s) + K_2 \Delta \tilde{\mathbf{u}}_k^*(s) \quad (17)$$

The Tustin transformation approximates the Laplace operator, s , in terms of the sampling shift operator, z per Ref. 9.

$$s = (2/T)(z - 1)/(z + 1) \quad (18)$$

Equation (17) then can be written as

$$\Delta \mathbf{u}_k = \left(\frac{2}{T} I + K_2 \right)^{-1} \left[\frac{2}{T} (I - K_2) \Delta \mathbf{u}_{k-1} - K_1 (\Delta \tilde{\mathbf{x}}_k + \Delta \tilde{\mathbf{x}}_{k-1}) + K_2 (\Delta \mathbf{u}_k^* + \Delta \mathbf{u}_{k-1}) \right] \quad (19)$$

This form of the proportional filter (PF) command augmentation system, which uses trapezoidal integration to generate $\dot{\mathbf{u}}$ from \mathbf{u} , was found to provide improved response when an initial control of $\Delta \mathbf{u}^*$ alone [as from Eq. (16)] caused unacceptably large transients.

Assuming that the pilot's commands can be interpreted as some linear combination of the state and control, a constant pilot command should result in constant state and control vectors,

$$\Delta \mathbf{y}^* = H_x \Delta \mathbf{x}^* + H_u \Delta \mathbf{u}^* \quad (20)$$

H_x and H_u define the command relationship, and the dimensions of $\Delta \mathbf{y}$ and $\Delta \mathbf{u}$ are equal. At equilibrium, $\Delta \mathbf{x}_{k+1} = \Delta \mathbf{x}_k$, so the combined solution of Eqs. (6) and (20)

leads to a direct solution for Δx^* and Δu^* in terms of Δy^* :

$$\begin{bmatrix} \Delta x^* \\ \Delta u^* \end{bmatrix} = \begin{bmatrix} (\Phi - I) & \Gamma \\ H_x & H_u \end{bmatrix}^{-1} \begin{bmatrix} 0 \\ \Delta y^* \end{bmatrix} \triangleq W^{-1} \begin{bmatrix} 0 \\ \Delta y^* \end{bmatrix} \quad (21a)$$

$$= S \begin{bmatrix} 0 \\ \Delta y^* \end{bmatrix} \quad (21b)$$

or

$$\Delta x^* = S_{11}(0) + S_{22}\Delta y^* \quad (21b)$$

$$\Delta u^* = S_{21}(0) + S_{22}\Delta y^* \quad (22)$$

As long as W is nonsingular, i.e., can be inverted, the partitions of S are well-defined, and the sampled-data regulators [Eqs. (10), (16), and (19)] can be written as,

Nonsingular Proportional

$$\Delta u_k = (S_{22} + K S_{12}) \Delta y_k^* - K \Delta x_k \quad (23)$$

Nonsingular Proportional Filter

(Forward Difference)

$$\begin{aligned} \Delta u_k = & S_{22}\Delta y_k^* + [TK_1 S_{12} - (I - TK_2)] \Delta y_{k-1}^* \\ & + (I - TK_2) \Delta u_{k-1} - TK_1 \Delta x_{k-1} \end{aligned} \quad (24)$$

Nonsingular Proportional Filter

(Tustin)

$$\begin{aligned} \Delta u_k = & \left(\frac{2}{T} I + K_2 \right)^{-1} \left[(K_1 S_{12} + K_2 S_{22}) (\Delta y_k^* + \Delta y_{k-1}^*) \right. \\ & \left. + \left(\frac{2}{T} I - K_2 \right) \Delta u_{k-1} + K_1 (\Delta x_k + \Delta x_{k-1}) \right] \end{aligned} \quad (25)$$

Unfortunately, S does not exist for some of the more interesting command variables, e.g., roll rate, because the state vector contains a pure integral of the command variable (pitch angle or roll angle). By definition, the integral cannot be constant when the command is a nonzero constant. As in the continuous-time case,¹ the problem can be solved by defining a quasi-steady equilibrium for a reduced-order system, treating the integral state as an "exogenous" forcing term that grows continuously as long as the command is constant. Equations (6) and (20) are partitioned as

$$\begin{bmatrix} \Delta x_1 \\ \Delta x_2 \end{bmatrix}_{k+1} = \begin{bmatrix} \Phi_1 & \Phi_2^1 \\ \Phi_2^2 & I \end{bmatrix} \begin{bmatrix} \Delta x_1 \\ \Delta x_2 \end{bmatrix}_k + \begin{bmatrix} \Gamma_1 \\ 0 \end{bmatrix} \Delta u_k \quad (26)$$

$$\Delta y^* = [H_{x1} \ 0] \begin{bmatrix} \Delta x_1^* \\ \Delta x_2^* \end{bmatrix} + H_u \Delta u^* \quad (27)$$

Δx_1 is the reduced-order state, and Δx_2 is the integral state. The quasi-steady equilibrium is defined as

$$\begin{aligned} \begin{bmatrix} \Delta x_1^* \\ \Delta u_1^* \end{bmatrix}_k &= \begin{bmatrix} (\Phi_1 - I) & \Gamma_1 \\ H_{x1} & H_u \end{bmatrix}^{-1} \begin{bmatrix} -\Phi_2^1 \Delta x_2^* \\ \Delta y^* \end{bmatrix}_k \\ &= S' \begin{bmatrix} -\Phi_2^1 \Delta x_2^* \\ \Delta y^* \end{bmatrix}_k \end{aligned} \quad (28)$$

and the integral state Δx_{2k} is propagated by

$$\Delta x_{2k}^* = \Delta x_{2k-1}^* + \Phi_2^2 \Delta x_{1k-1}^* \quad (29)$$

As an example, a sideslip angle/roll command vector yields the following set point at the VRA's 105 KIAS flight condition:

$$\begin{bmatrix} \Delta r^* \\ \Delta \beta^* \\ \Delta p^* \end{bmatrix}_k = \begin{bmatrix} 0.18 \\ 0 \\ 0 \end{bmatrix} \Delta \phi_k^* + \begin{bmatrix} -0.47 & .004 \\ 1 & 0 \\ 0 & 1 \end{bmatrix} \begin{bmatrix} \Delta \beta^* \\ \Delta p^* \end{bmatrix}_k \quad (30)$$

$$\begin{bmatrix} \Delta \delta R^* \\ \Delta \delta A^* \end{bmatrix}_k = \begin{bmatrix} -0.2 \\ -.01 \end{bmatrix} \Delta \phi_k^* + \begin{bmatrix} 1.0 & -.06 \\ 0.55 & 0.31 \end{bmatrix} \begin{bmatrix} \Delta \beta^* \\ \Delta p^* \end{bmatrix}_k \quad (31)$$

Note that the steady-state roll angle commands the steady-state yaw rate to coordinate the turn.

The singular command augmentation controllers then are defined as Eq. (29) plus the following:

Singular Proportional

$$\begin{aligned} \Delta u_k = & (S_{22} + K_1 S_{12}') \Delta y_k - K \Delta x_k \\ & + [K_2 - (S_{21}' - K_1 S_{11}') \Phi_2^1] \Delta x_{2k}^* \end{aligned} \quad (32)$$

where the K of Eq. (10) is partitioned as $[K_1 \ K_2]$ to be conformable with Δx_1 and Δx_2 .

Singular Proportional Filter

(Forward Difference)

$$\begin{aligned} \Delta u_k = & S_{22}' \Delta y_k^* + [(TK_2 - I) S_{22}' + TK_{11} S_{22}'] \Delta y_{k-1}^* \\ & - S_{21}' \Phi_2^1 \Delta x_{2k}^* + (I - TK_2) \Delta u_{k-1} - TK_1 \Delta x_{k-1} \\ & + \{ [(I - TK_2) S_{21}' - TK_{11} S_{11}'] \Phi_2^1 + TK_{12} \} \Delta x_{2k-1}^* \end{aligned} \quad (33)$$

with the K_1 of Eq. (16) partitioned as $[K_{11} \ K_{12}]$.

Singular Proportional Filter

(Tustin)

$$\begin{aligned} \Delta u_k = & \left(\frac{2}{T} I + K_2 \right)^{-1} \left\{ \left(\frac{2}{T} I - K_2 \right) \Delta u_{k-1} \right. \\ & - K_1 (\Delta x_k + \Delta x_{k-1}) + (K_{11} S_{12}' + K_{21} S_{22}') \\ & \times (\Delta y_k^* + \Delta y_{k-1}^*) + [-K_{11} S_{11}' + K_{21} S_{21}'] \Phi_2^1 + K_{12} \\ & \left. + K_{22} \right\} (\Delta x_{2k}^* + \Delta x_{2k-1}^*) \end{aligned} \quad (34)$$

with K_2 [Eq. (19)] also partitioned as $[K_{21} \ K_{22}]$. These control laws have the Type 1 property with respect to the singular command variable because they contain integral error terms formed by $(\Delta x_2 - \Delta x_2^*)$.

The nonsingular PF controller can be transformed to a Type 1 proportional-integral (PI) structure

$$\Delta u_k = \Delta u_{k-1} - C_1 (\Delta x_k - \Delta x_{k-1}) - C_2 (H_x \Delta x_{k-1} - \Delta y_k^*) \quad (35)$$

(with $H_u = 0$) by defining

$$[C_1 \ C_2] = [TK_1 \ TK_2] S \quad (36)$$

as in Ref. 8.† In the singular case, the PI controller takes advantage of the natural Type 1 characteristic of the PF control law. Equation (36) is applied to the reduced-order model, transforming K'_1 and K'_2 to C'_1 and C'_2 , and the equivalent singular Type 1 control law is written as⁴

$$\begin{aligned} \Delta u_k = & \Delta u_{k-1} - (S'_{21} + C_{11}S'_{11})\Phi_2^l(\Delta x_{2k}^* - \Delta x_{2k-1}^*) \\ & + (S'_{22} + C_{11}S'_{12})(\Delta y_k^* - \Delta y_{k-1}^*) \\ & + (C_{11}\Phi_2^l - TK_{12})(\Delta x_{2k-1}^* - \Delta x_{2k-2}^*) \\ & + C_2(\Delta y_{k-1}^* - \Delta y_{k-2}^*) - C_{11}(\Delta x_{1k} - \Delta x_{1k-1}) \end{aligned} \quad (37)$$

This controller was simplified, as in Ref. 4, for flight testing.

Command Augmentation Control Laws

During flight testing of CAS-4, the evaluation pilot's center stick and foot pedals commanded desired values of the motion variables. For the sideslip angle/roll rate (β, p) modes, the stick commanded p^* , and the pedals commanded β^* , so the command relationship [Eq. (20)] was

$$y^* = \begin{bmatrix} \beta^* \\ p^* \end{bmatrix} = \begin{bmatrix} 0 & 1 & 0 & 0 \\ 0 & 0 & 1 & 0 \end{bmatrix} \begin{bmatrix} r \\ \beta \\ p \\ \phi \end{bmatrix} + \begin{bmatrix} 0 & 0 \\ 0 & 0 \end{bmatrix} \begin{bmatrix} \delta R \\ \delta A \end{bmatrix} \quad (38)$$

The β, p modes used both Type 0 and Type 1 controllers, Eqs. (33) and (37). Experiments also were conducted with lateral acceleration (a_y) and yaw rate (r) replacing β as a command variable.⁴ In addition, the digital DEL mode provided direct feeds from stick and pedals to aileron and rudder.

The present discussion focuses on the β, p modes, except as noted. The β, p controller was tested with four gain sets derived from the continuous-time linear-quadratic weighting factors, i.e., the diagonal elements of Q_1 , Q_2 , and R , given in Table 1. The Mode D control law also was shaped by β and p weightings of 20 and 0.25, respectively. The progression from Mode A to C reflects increasing penalty for control usage; Mode D continues this trend through the effects of reduced Q_1 and state-rate weighting. Overshoots and the handling qualities parameter " ϕ/β " are minimal,§ and rise time steadily increases for both command inputs.

Perturbation gains (K_1 and K_2) for Modes A and C, with 10 per s sampling rate, are shown in Table 2. These also reflect the effect of increasing control weighting.

Table 3 summarizes Mode A closed-loop natural frequencies ω_n , damping ratios ζ , real roots λ , and the two largest eigenvector magnitudes v_1 and v_2 for each dynamic mode. These equivalent continuous-time parameters are derived from the eigenvalues and eigenvectors of F_{CL} , where F_{CL} is defined as,¹²

$$F_{CL} = \frac{1}{T} \ln \Phi_{CL} = \frac{1}{T} [\Phi_{CL} - I] - \frac{1}{2} (\Phi_{CL} - I)^2 + \dots \quad (39)$$

and Φ_{CL} is the closed-loop state transition matrix. For comparison, the open-loop values also are given. The unaugmented VRA has a lightly damped Dutch Roll oscillation, a quick roll mode, and a nearly neutral spiral mode. The closed-loop mode shape is decidedly different

Table 1 Weightings and step response characteristics for β, p modes

		Mode			
		A	B	C	D
State	r	250	30	25	10
	β	5000	250	30	10
Weightings	p	100	30	10	0
	ϕ	25	15	.5	0
Control	δR	15	33	15	15
Weightings	δA	15	33	15	15
Rate	$\delta \dot{R}$	1	1	1	1
Weightings	$\delta \dot{A}$	1	1	1	1
p Command Response					
Rise Time, sec		.2	.23	.37	.96
Overshoot, %		7.4	7.4	3.6	2.8
β Command Response					
Rise Time, sec		.82	1	1.83	2.37
Overshoot, %		.06	.21	.80	1.20
" ϕ/β "		.19	.10	.24	.22

Table 2 Type 0 gains for β, p modes, sampling rate = 10 per s

		Mode			
		A		C	
		δR	δA	δR	δA
K_1	r	-10.48	.63	-2.23	.43
	β	11.21	-3.3	-3.48	-2.2
	p	.40	1.5	.10	.43
	ϕ	1.70	2.6	.15	.66
K_2	δR	14.25	.02	7.07	-.05
	δA	1.01	11.9	.36	6.68

Table 3 Eigenvalues and eigenvectors of β, p Mode A and the unaugmented VRA

β, p Mode A			Unaugmented VRA		
$\omega_n(\lambda)$, rad/s	ζ	v_1, v_2	$\omega_n(\lambda)$, rad/s	ζ	v_1, v_2
14.6	.75	$p, \delta A$	(-6.6)	-	p, ϕ
9.9	.68	$\delta R, r$	2.6	.20	r, p
(-4.4)	-	$r, \delta R$	-	-	-
(-0.6)	-	ϕ, p	(-0.007)	-	ϕ, r

from the open-loop case, although all modes are well-behaved. The roll mode coalesces with the aileron filter dynamics, while the Dutch roll mode combines with the rudder filter dynamics. The spiral mode becomes a purer rolling motion.

Mode A and C responses to sideslip and roll rate step inputs are shown in Figs. 1 and 2. These digital simulations exhibit well-controlled transients and a high degree of steady-state decoupling. Commanded β and p responses are precise. The β command results in a flat turn, and the p command provides a coordinated turn using conventional pilot inputs. For β commands, the sharp p transient is followed by a steady return to zero roll rate. For p commands, there is a residual β perturbation associated with the quasi-steady-state approximation [Eqs. (28) and (29)]. This "hangoff" is nulled completely in the Type 1 realization.⁴ The PI version of the β, p Mode C controller has identical p command response and slightly slower β command response (rise time = 2.1 s).

The Type 1 PI controller is tolerant of stability- and control-parameter variations. The PF and PI controllers are

†This result was derived in {11}.

§" ϕ/β " represents the ratio of roll and sideslip angle component magnitudes in the Dutch roll eigenvector.

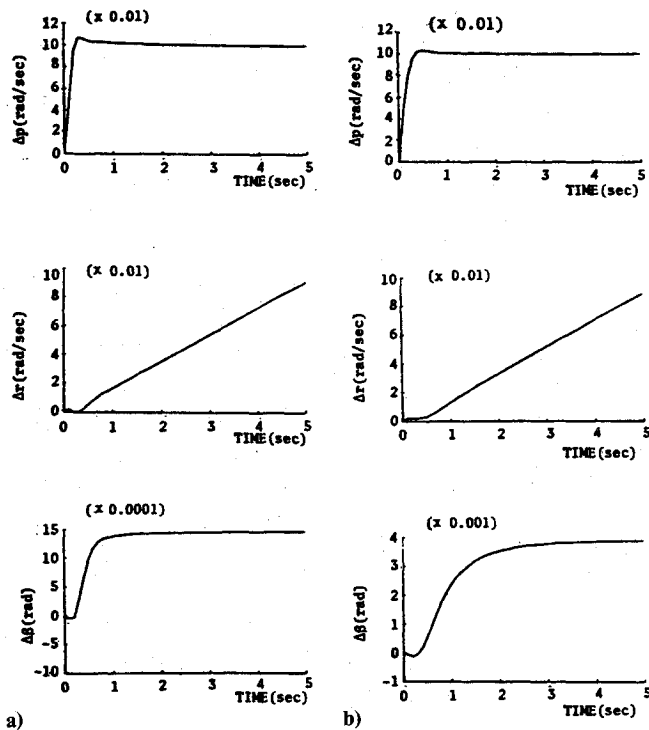


Fig. 1 Response to command roll rate, β, p : a) Mode A; b) Mode C.

compared in Fig. 3, with 25% variations in L_p and $N_{\delta R}$ from design values. Reduced roll damping (L_p) causes an overshoot in both p responses. PF and PI responses both converge to the proper value because both possess the Type 1 property for roll rate commands (Fig. 3a); however, the PI controller's convergence is quicker. The PF controller's sideslip angle response does not have the Type 1 property, so there is considerable hangoff with 25% decrease in rudder effect ($N_{\delta R}$) (Fig. 3b); the PI controller quickly nulls the error under similar circumstances.

Operational Control Structure and Preflight Simulation

Micro-DFCS and CAS-4

The primary tasks of the Micro-DFCS were to accept analog information from aircraft sensors (including the evaluation pilot's controls), to calculate the control laws, and to send analog commands to the VRA's control effectors at periodic instants in time. As described in Refs. 2 and 3, the Model 1 Micro-DFCS consisted of a flight control computer unit (FCCU) and a control-display unit (CDU). The FCCU contained six Multibus boards for analog input, analog output, central processing, arithmetic processing, main memory storage, and backup memory storage. Although the 8085 central processor used 8-bit data words, all mathematical operations used 32-bit floating-point format. Analog inputs and outputs were quantized at the 12-bit level.

The CAS-4 flight control computer program contained three sets of routines.^{2,3} The Executive Routines provided initialization, CDU interface, and memory check. The Utility Routines included data conversion, error detection, status driver, math driver, mode change, timer/sampling rate selection, variable pure delay, variable output quantization, and output limiting. The Flight Control Routines provided mode set up for each mode change and interrupt service at each control sampling instant. The Executive Routines required 363 bytes of memory, while the Utility Routines were stored in 1939 bytes. The remaining 4549 bytes of CAS-4 contained the Flight Control Routines. These consisted of

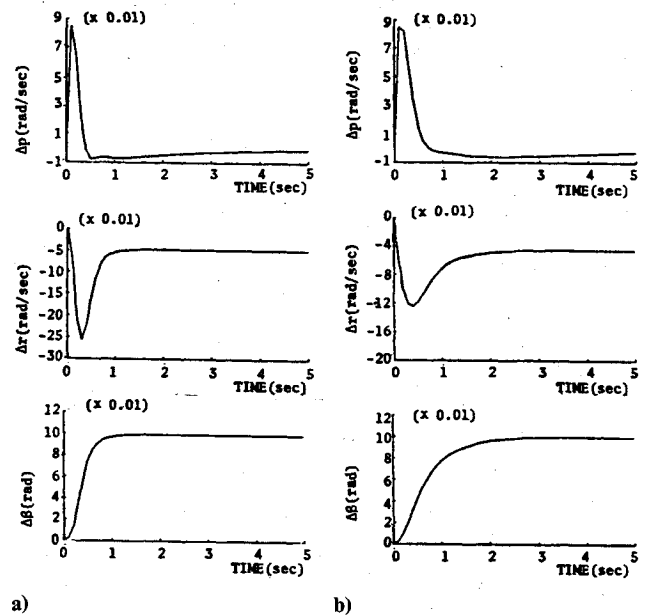


Fig. 2 Response to commanded sideslip angle, β, p : a) Mode A; b) Mode C.

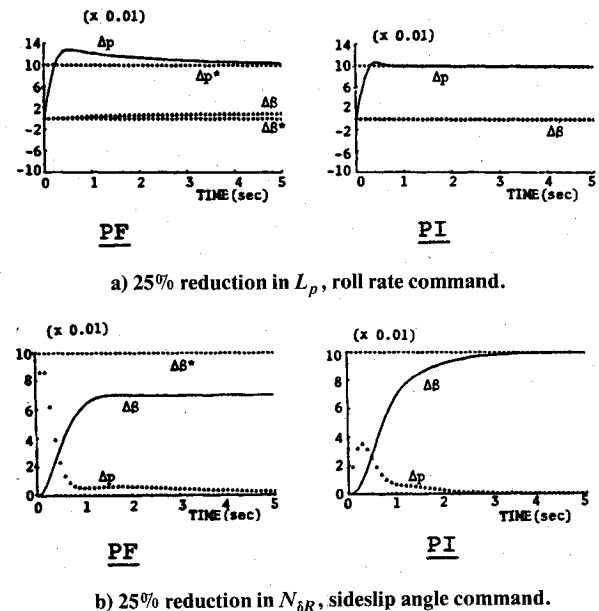


Fig. 3 Effects of parameter variations on PF and PI controller response, β, p mode.

setup and service routines for four command modes and thirteen sets of gains. Thus, it was possible to switch rapidly from one mode and set of gains to another in flight. In addition, alternate gain sets could be entered through the CDU.

The computation time of the digital DEL mode was 8 ms; the PF controllers executed in 37 ms. The PF logic could be structured to reduce the transport lag between analog inputs and outputs to 12 ms. This was accomplished by computing only those terms that depended on the current input during the input-output interval and all the lagged terms in the control law during the output-input interval.

Flight Testing of the Digital Control System

Several VRA flights were conducted in this investigation. The first series of flights were engineering tests flown by

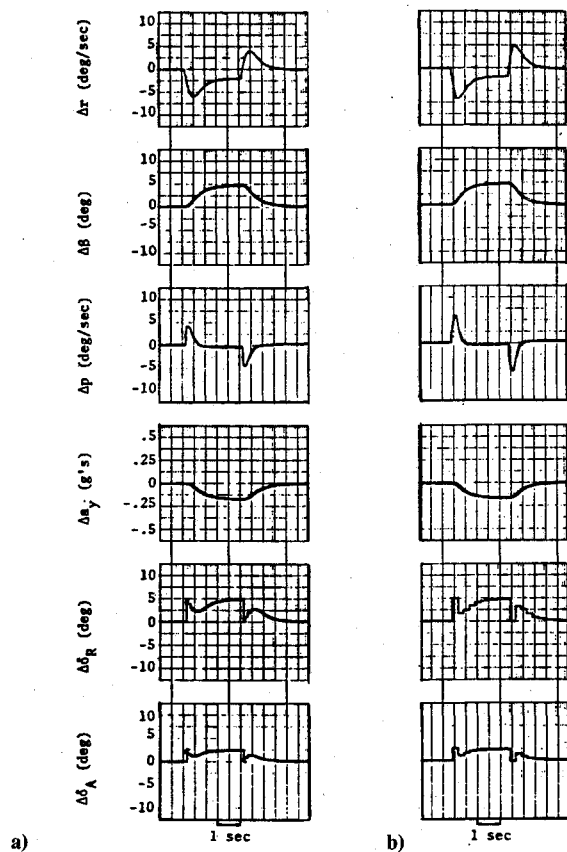


Fig. 4 Effects of sampling rate on β, p Mode C response to sideslip angle command; a) 10 sps; b) 4 sps.

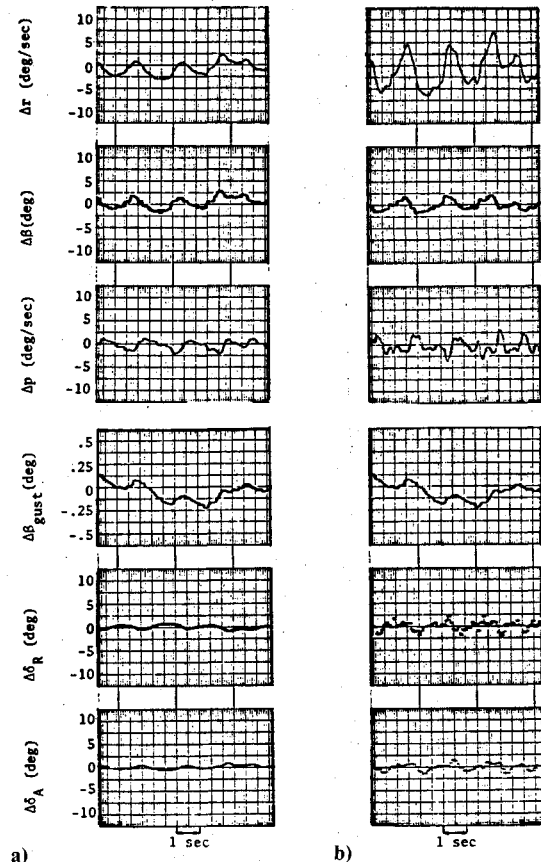


Fig. 5 Comparison of random disturbance responses of β, p Mode C control laws; a) PF controller; b) PI controller.

Princeton Pilots A and B. General observations were made regarding the control of attitude and flight path in cruising flight. The second series included tracking and landing approach tasks flown by U.S. Navy Test Pilots C and D. Various tracking tasks were performed, as described below. The landing approach was made using visual guidance from an aircraft carrier approach mirror and an angle-of-attack meter/indexer, as in Ref. 3. All pilots provided commentary, and Pilots C and D used the Cooper-Harper Handling Qualities Rating (HQR) scale as a measure of pilot opinion. The Cooper-Harper scale¹³ assigns numerical values between 1 and 10 to each configuration tested, with 1 indicating highly desirable flying qualities and 10 indicating deficiencies great enough to cause loss of control. The effects of direct-mode digital control on pilot opinion are reported in Ref. 14; pilot opinions of CAS-4 closed-loop modes are presented below.

CAS-4 Step Response

Telemetry recordings of the aircraft's response to step inputs confirmed ground simulation trends. Response to roll rate (lateral stick) command for the β, p Mode C is shown in Fig. 4. The PF and PI traces are very similar, but the PI response was marked by overshoot and continuing high-frequency oscillation. Sideslip angle response (not shown) was negligible in all cases. Response to sideslip angle (foot pedal) command is shown in Fig. 4. The r and p transients were more peaked at 4 sps than at 10 sps, and the residual oscillations seen in Fig. 4 reappear in the PI result. Roll angle response was nil in all cases.

Pilot Opinions of Handling Qualities

The engineering flight tests provided the evaluations summarized in Table 4. Sampling rate was 10 per s, except as

noted. Pilots A and B preferred β, p Mode C and a_y, p Mode B to the other Modes. Reducing the β, p sampling rate to 8 per s had little effect on flying qualities; at 6 sps, roll control was noticeably more abrupt, and at 5 per s, sideslip "jerkiness" became apparent. At 4 sps, closed-loop control resolution was bothersome but less so than for DEL control at the same sampling rate.

Pilot C, whose experience had been gained primarily in anti-submarine warfare aircraft, flew the VRA with CAS-4 in five tasks. Task 1 involved low-gain lateral maneuvering, with 45 deg bank-to-bank turns and large control inputs. Task 2 consisted of rapid 3 deg heading changes (± 1 deg), with bank angles of 10 deg or less. This task was similar to maneuvering for air-to-air refueling. Foot pedals were not used unless required for turn coordination. Task 3 required track to be maintained while performing a slip, and Task 4 involved changing track in the slip. Task 5 was directed toward 30 deg (or greater) flat turns, with final heading hold (± 3 deg). This maneuver is representative of heading change in a surveillance aircraft. Sampling rates were 10 per s, except as noted. Pilot C's evaluation is summarized by Table 5.

For normal maneuvering (Tasks 1 and 2), Pilot C preferred the direct modes to the closed-loop modes, and was able to discern an improvement when the sampling rate was increased from 10 to 20 per s. The foot pedals were used very little in these cases. Choosing among the closed-loop modes, Pilot C showed a definite preference for the a_y, p modes, and he gave his best ratings to a_y, p Mode B. In other words, he preferred faster response than Pilots A and B. Tasks 3 to 5 could not be accomplished easily with the direct mode; the Task 5 HQR of 6 falls well above the ratings for the best closed-loop modes.

Ratings for β, p Mode C deteriorated as sampling rate decreased. This was not the result of poorer transient response but of increased sampling delay. On the average, pilot command inputs occur halfway between sampling instants;

Table 4 Pilot A and B evaluations of CAS-4 for conventional operations

β, p Mode A – Acceptable response, although yaw is jerky and sensitive to β commands. Roll response good with no adverse yaw. Rate of turn smoothly follows roll rate.
β, p Mode B – No difference in roll response. Sideslip response better due to perceived lower N_β .
β, p Mode C – No noticeable difference in roll response. Sideslip angle response is softer than Mode B but very good, with no adverse effect in roll. The preferred configuration.
β, p Mode D – Roll response considered acceptable but rated poorer due to slower response time. No noticeable difference in yaw response.
β, p Mode C (PI) – Very jerky hands-off response, especially in yaw. Seems to have faster response than PF version. Ride quality very sensitive to turbulence. No heading changes associated with turbulence response, just high frequency disturbances. Excessive yaw stiffness. Roll response faster than desired but acceptable.
a_y, p Mode A – Response appeared similar to β, p Mode B.
a_y, p Mode B – Response appeared similar to β, p Mode C.
β, p Mode C (8 sps) – No degradation noted in roll or yaw control. Slight abruptness in start and stop of roll maneuver.
β, p Mode C (6 sps) – Yaw response same as 10 sps. Abruptness more noticeable in roll.
β, p Mode C (5 sps) – Jerkiness in yaw is apparent but not objectionable. Roll response is erratic. Time lag is noticeable, depends on timing of input.
β, p Mode C (4 sps) – Roll objectionable, due to ratchet-type control movements and response. The same is true in yaw response but is not objectionable. Response delay acceptable in yaw, annoying in roll.
DEL (10 sps) – Same response as continuous-time, open-loop response.
DEL (4 sps) – Jerkiness of controls main objection. Thumping of control surfaces very apparent. Prefer closed-loop control at low sampling rates due to improved turbulence response.

Table 5 Handling qualities ratings of Pilot C

Control Mode	Task number				
	1	2	3	4	5
$\beta, p-A$	4.5	4.0	5.0	5.0	5.0
$\beta, p-B$	3.0	3.3	4.0	4.0	4.0
$\beta, p-C$	3.0	4.0	3.0	4.0	2.5
$\beta, p-D$	4.5	5.0	—	—	—
$a_y, p-A$	3.5	4.0	4.0	4.0	4.0
$a_y, p-B$	2.8	2.8	3.0	3.0	3.0
$a_y, p-C$	4.0	4.0	3.0	4.0	4.0
$\beta, p-C(8)$	4.0	4.0	—	—	—
$\beta, p-C(6)$	5.0	4.5	—	—	—
$\beta, p-C(5)$	6.0	4.5	—	—	—
$\beta, p-C(4)$	7.5	7.0	—	—	—
DEL (10)	2.5	2.5	—	—	6.0
DEL (20)	2.0	2.0	—	—	—

Table 6 Handling qualities ratings of Pilot D

Control Mode	Task number			
	1a	1b	2a	2b
$\beta, -A$	5.0	6.0	—	—
$\beta, p-B$	3.0	3.0	—	—
$\beta, p-C$	3.0	2.5	3.0	3.0
$\beta, p-D$	3.0	4.0	—	—
$a_y, p-A$	4.0	5.0	—	—
$a_y, p-B$	3.0	3.0	—	—
$a_y, p-C$	4.0	4.0	—	—
$\beta, p-C(8)$	2.5	4.0	5.0	5.0
$\beta, p-C(6)$	2.5	2.0	3.0	3.0
$\beta, p-C(5)$	4.0	5.0	5.0	6.0
$\beta, p-C(4)$	4.0	4.0	6.0	7.0
DEL (10)	4.0	4.5	—	—
DEL (20)	4.0	3.0	—	—

hence, there is an equivalent transport delay associated with digital control.³

Pilot D, with fighter aircraft experience, flew the VRA with CAS-4 in two tasks, each of which was subdivided in two parts. Task 1 involved acquisition and tracking of fixed objects on the ground. The acquisition phase (1a) began by selecting a point 35-45 deg off the nose and pulling the aircraft up to a 10 deg nose-high attitude. At 75 KIAS, he rolled into a 10 deg dive, accelerating to 105 KIAS and attempted to center the object in the field of view (± 5 mils). The tracking phase (1b) continued for 15-20 s, holding airspeed and using the best combination of stick and pedals to maintain pointing. Task 2 is identified as field carrier landing practice (FCLP). The approach phase (2a) began at 650 ft altitude about 1.5 nm from the runway. A 3.5-deg approach was made at 86 KIAS. The "close-in" phase (2b) began at 0.5 nm from the landing mirror and ended with a waveoff at 10-15 ft altitude. Pilot D's evaluation is summarized by Table 6.

Pilot D generally liked the closed-loop modes more than the direct mode, and he was able to adapt to slow sampling rate during the tracking task. Sampling delays degraded his ratings, but only for rates below 6 per s. Ratings for the β, p and a_y, p modes were equivalent, with a preference for the same speed of response preferred by Pilots A and B.

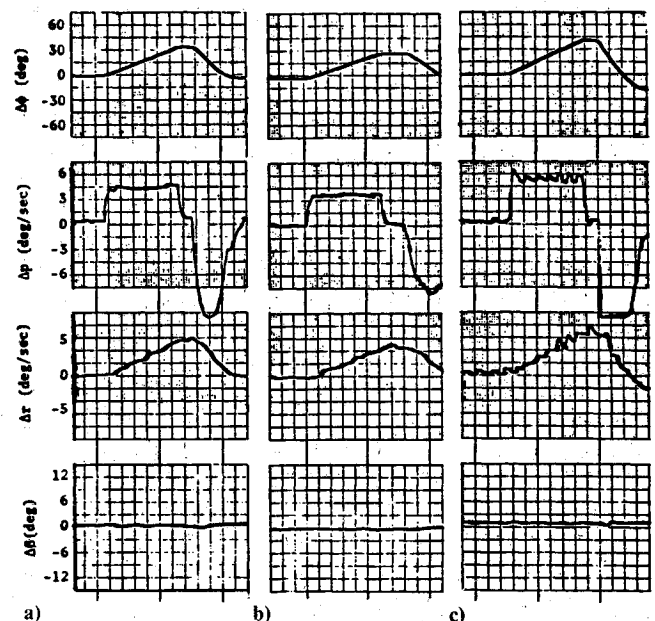


Fig. 6 β, p Mode C roll rate step response from flight test; a) PF, 10 sps; b) PF, 4 sps; c) PI, 10 sps.

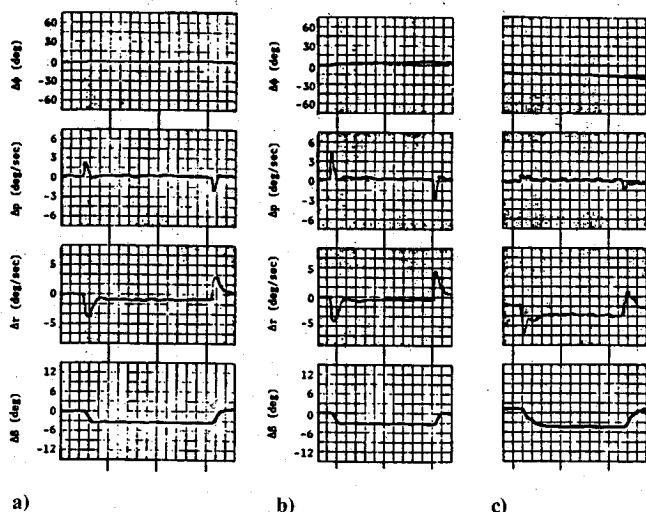


Fig. 7 β, p Mode C sideslip angle step response from flight test; a) PF, 10 sps; b) PF, 4 sps; c) PI, 10 sps.

Decreasing sampling rate had greater impact on landing approach than on tracking. Pilot D also sensed an improvement in the higher-rate direct mode.

Conclusion

Lateral-directional control laws were successfully designed and tested in flight. Flight tests showed that major closed-loop response features were largely unaffected by the choice of sampling rate (down to 4 sps), although sampling delay of pilot inputs degraded handling qualities ratings. The closed-loop digital control laws provided improved command response and exhibited improved steady-state decoupling, compared to the VRA's open-loop dynamics, at all sampling rates investigated. Ground simulations and flight testing showed that the Type 1 system, which was designed to have a step response that was virtually identical to an equivalent Type 0 system, was extremely sensitive to noise inputs and turbulence, although it was tolerant of large variations in aircraft parameters. The Type 0 controllers provided satisfactory performance in ground test and in flight, but their steady-state performance could be affected by aircraft parameter variations.

Acknowledgment

This research was sponsored by the Office of Naval Research, Arlington, Va., under Contract No. N00014-78-C-0257. Jerry LaReau, USN, Winston Copeland, USN, Barry Nixon, and George Miller served as evaluation pilots for this program. The cooperation of the Naval Air Test Center, Patuxent River, Md., is gratefully acknowledged.

References

- Stengel, R.F., "Equilibrium Response of Flight Control Systems," *Automatica*, Vol. 18, May 1982, pp. 343-348.
- Stengel, R.F., "Digital Flight Control Research Using Microprocessor Technology," *IEEE Transactions on Aerospace and Electronic Systems*, Vol. AES-15, May 1979, pp. 397-404.
- Stengel, R.F., and Miller, G.E., "Flight Tests of a Microprocessor Control System," *Journal of Guidance and Control*, Vol. 3, Nov.-Dec. 1980, pp. 494-500.
- Atzhorn, D., "Digital Command Augmentation for Lateral-Directional Aircraft Dynamics," Office of Naval Research, Rept. No. ONR-CR-300-003-2 (also M.S.E. Thesis, Princeton University), May 1981.
- Binnie, W.B., and Stengel, R.F., "Flight Investigation and Theory of Direct Side-Force Control," *Journal of Guidance and Control*, Vol. 2, Nov.-Dec. 1979, pp. 471-478.
- "Military Specification, Flying Qualities of Piloted Airplanes," MIL-F-8785C, USAF ASD/ENESS, Wright-Patterson AFB, Dayton, Ohio, Nov. 1980.
- Dorato, P. and Levis, A.H., "Optimal Linear Regulators: The Discrete-Time Case," *IEEE Transactions on Automatic Control*, Vol. AC-16, Dec. 1971, pp. 613-620.
- Stengel, R.F., Broussard, J.R. and Berry, P.W., "Digital Controllers for VTOL Aircraft," *IEEE Transactions on Aerospace and Electronic Systems*, Vol. AES-14, Jan. 1978, pp. 54-63.
- Tustin, A., "A Method of Analyzing the Behavior of Linear Systems in Terms of Time Series," *Journal of the IEE*, Vol. 94, Pt IIa, 1947, pp. 130-142.
- Stengel, R.F., Berry, P.W., and Broussard, J.R., "Command Augmentation Control Laws for Maneuvering Aircraft," AIAA Paper No. 77-1044, Aug. 1977.
- Broussard, J.R. and Safonov, M., "Design of Generalized Discrete Proportional-Integral Controllers by Linear-Optimal Control Theory," The Analytic Sciences Corp., TIM-804-1, Oct. 1976.
- Stengel, R.F., Broussard, J.R., and Berry, P.W., "Digital Flight Control Design for a Tandem-Rotor Helicopter," *Automatica*, Vol. 1, July 1978, pp. 301-311.
- Cooper, G.E. and Harper, R.P., Jr., "The Use of Pilot Rating in the Evaluation of Aircraft Handling Qualities," NASA TN D-5153, April 1969.
- Stengel, R.F. and Miller, G.E., "Pilot Opinions of Sampling Effects in Lateral-Directional Control," *Proceedings of the 16th Annual Conference on Manual Control*, Cambridge, Mass., May 1980.